Frequency Domain Near-IR Light Studies of Turbid Media with Means to Detect Breast Cancer

Diploma Paper
by
Heléne Tagesson

Lund Reports on Atomic Physics, LRAP-180
Lund, July 1995

Abstract

This paper describes a phase-shift technique to enhance contrasts in optical trans-illumination of turbid media. In this technique a modulated diode laser is used to illuminate a sample. The AC-component of the detected signal is then mixed with the modulation signal, and a DC-signal proportional to the cosine of the phase lag between these two signals is obtained. Multiple scattering of the light in the turbid medium will give rise to light with different path lengths within the medium contributing to the signal. Different path lengths of light will result in a phase shift of the signal, and the multiple scattering will also give rise to a demodulation of the signal. By detecting the phase shift and the demodulation, regions in a probed medium, with optical properties different from the bulk volume, could be identified. The technique has applications in light scanning of female breasts in order to detect breast cancer. The tissue phantom used in this study consisted of a solution of Intralipid, which is a liquid with optical properties similar to those of tissue. A glass rod or a black plastic rod in the liquid, simulating abnormalities, e.g. tumours, gave detectable changes on the signal.

Contents

1 Introduction

Breast cancer is the most frequent malignant tumour in women, and causes more deaths than any other cancer [1]. In Sweden about 8% of the female population will suffer from this disease during their life time [2]. The earlier the cancer is detected the better are the chances for a successful treatment, and hence it is important to find a reliable and efficient tumour detection method. Mammography is the method mainly used today. It is said to reduce mortality by about 30% among examined women [1]. There are however disadvantages with mammography: e.g. the potential risk of inducing cancer when using ionizing radiation and the discomfort of compression of the breast during examination. Another problem is that 7% of all tumours are not seen on a mammogram, and the corresponding figure for women below 50 years is as high as 22% [3]. It is therefore desirable to find an alternative or complement to mammography.

The purpose of this project has been to investigate light transillumination, where a laser beam illuminates a spot on one side of the breast and the light exiting on the opposite side is analysed. Published results indicate that tumour tissue is characterized by a lower scattering coefficient and a higher absorption coefficient than healthy breast tissue. These differences in optical properties make it possible to detect tumours. Before being able to fully develop the transillumination method, further investigations of the optical properties of tissue have to be performed. Especially, it is desirable to develop a method with high enough spatial resolution to identify small early tumours. This work was performed to being able to locally better judge the potential of the frequency domain optical transillumination method for breast cancer identification.

1.1 Breast Cancer

Cancer is the common name for all diseases caused by uncontrolled growth of cells in the body. When the cancer cells start to multiply, they form a tumour which can infiltrate and destroy surrounding tissue. There are two kinds of tumours: benign and malignant ones. The benign tumours grow slowly and are clearly defined. They are harmful only if they exert pressure on surrounding organs. The malignant tumours, on the other hand, grow more rapidly and infiltrate the surrounding organs. They produce toxic substances which may influence the whole organism, and will be harmful if they are left untreated. These tumours also shed cells that can be transported to other organs by blood and lymph, and form metastases there. The earlier the cancer is detected, the less will it have spread in the body and the better the chances for successful treatment.

The female breast has a very complex anatomy and no two women have exactly the same breast physiology, which explains why it is so difficult to find a simple and precise breast imaging method. The breast is composed of skin, fat, glandular tissue and connective tissue. During pregnancy and lactation the breast structure changes considerably, but there is also a periodic variation in the structure due to the female hormone cycle. Younger women have more dense breasts than elder ones, and at menopause a gradual replacement of the glands by fat takes place. Breast cancer is uncommon before the age of 30, 95% of detected cancers appear after the 40th year and the average onset age is about the 56th year [4, 2]. The biology and site of the

breast cancer varies widely, but 35-50% of the tumours develop in the upper outer quadrant of the breast [4]. Breast tumours require on average about four years to grow from a diameter of 2 mm to a diameter of 10 mm [4].

The incidence rate varies in different countries, but this is probably due to different environmental aspects rather than to racial differences. Asian women for example develop cancer less often than American women, but the Asian women in the USA are as likely to get cancer as other racial groups [1]. A common conception is that smoking should raise the risk of developing breast cancer, which has not been proven [1]. Alcohol on the other hand does; drinking one drink every day has been shown to increase the risk [1]. Another risk factor which has been discussed, is the birth control pill. It is, however, hard to tell whether modern birth control pills with lower oestrogen content increase the risk or not, as the women who have developed breast cancer today, took pills with more oestrogen. At the beginning of the century it was already known that nuns and unmarried women were more likely to develop breast cancer. This is most likely due to the fact that pregnancies and lactation decrease the risk. However, the protective effects of pregnancy decrease as the woman becomes older when bearing her first child. This is a fact that probably will increase the breast cancer in our society, where women wait to bear children. The period of a woman's menstruation is also important; early menarche and late menopause are risk factors for breast cancer.

The most important risk factor is however if relatives have had cancer. The risk then increases 2 to 4 times [1]. Some people in this risk group have the gene ataxia-telangiectasia, which is a recessive gene. People heterozygous for this gene make up 1% of the general population, and they have an excess risk for developing cancer, especially breast cancer [5]. Apart from this risk of developing cancer, they are also very sensitive to ionizing radiation. Therefore it is important to find reliable alternatives to diagnostic X-rays. In the case of mammography, the risk of inducing cancer may exceed the benefits of early detection.

1.2 Treatment Modalities

Four thousand year old hieroglyphs represent the oldest known descriptions of breast cancer (Fig. 1.1). At that time the entire breast was amputated in an operation taking just a few seconds. An open wound was all that was left, and the woman often died from an infection in the wound. Other treatments used were impositioning of hands and prayers. There was not much progress in the treatment methods until radiation therapy was invented at the end of the 19th century [1].

There are three principal methods of treatment today: surgery, chemotherapy and radiation therapy. Which method to be chosen, depends on the state of the tumour and the patient. Limited surgery in combination with radiation therapy can be used for tumours with a diameter less than 4 cm, which include 80% of all breast cancers [4]. The tumour and a wide margin of tumour-free tissue is then removed. The 5-year survival rate is as high as 90%, when this method is used [4]. If lymph node metastases have developed, chemotherapy is also added. About 40% of all breast cancers have lymph node metastases, and for them a second operation is often needed [4]. The

recurrence rate during the first five years is here 50-70% compared with only 25% for cancers without lymph node metastases [4]. If the cancer is left untreated, the 5-year survival rate is as low as 18% and the average survival time is only 2.5 years [4].

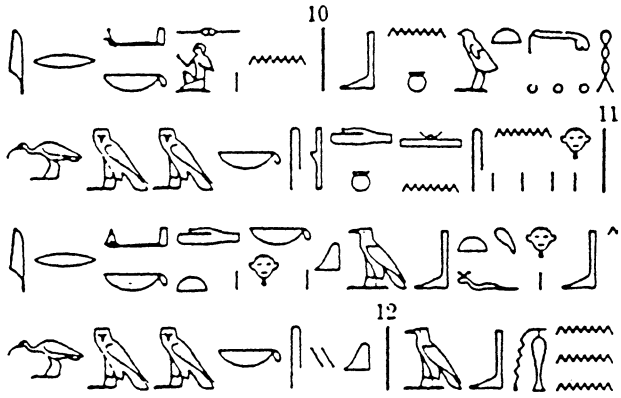

Fig 1.1 *The oldest known description of breast cancer - four thousand year old hieroglyphs. (From Ref. [1].)*

Two thirds of all breast cancers can be completely cured [2]. The earlier the tumour is detected, the greater are the chances for successful treatment and the smaller is the surgical operation needed. Loosing a breast is a great loss and can lead to mental sufferings for a woman, even if she is cured from the cancer itself. Therefore it is desirable to remove as little of the breast as possible. In order to do so, it is important to find safe and efficient detection methods.

1.3 Detection Methods

Today a majority of breast cancers are detected by the women themselves. The average size of the detected tumour is 2.5 cm in diameter and about 50% of the cysts have already metastasized to the lymph nodes [6]. A combination of self-examination and a harmless mass-screening would be desirable to attain earlier detection in order to reduce the mortality.

Current methods for breast imaging are based on X-rays, ultrasound, heat, light and magnetism. Despite the obvious attraction for nonionizing techniques, they all suffer shortcomings when it comes to expense, portability and examination-time.

1.3.1 Mammography

The method generally used for mass-screening today is mammography. It has been used for a long time and is well known. The first *in vivo* mammography was performed by Warren in 1930 and by about 1960 a reliable diagnostic technique had been developed by Egan [6]. Since then the method has been improved and the X-ray dose required has been lowered.

Today's methods are based on low-dose X-rays and vigorous compression of the breast (see Fig. 1.2). The estimated single exposure dose is about 1.4 mGy and the examination just requires a few minutes [1]. The breast is compressed to a thickness of a few centimeters between two glass plates. A photographic plate is placed on one side and the other side is radiated with X-rays. The tumour absorbs more of the X-rays than healthy tissue. The tumour is thus visible on a mammogram as a less exposed region. The breast is exposed at two different angles to increase the probability of detecting hidden tumours, but still about 7% of all cancers are not seen on a mammogram [3]. Examination of the mammograms requires experienced medical staff. It has been proven that 20% more tumours are found if two different doctors look at the same mammogram. This is done in Lund, but some hospitals do not do so, as they consider it being too expensive [7].

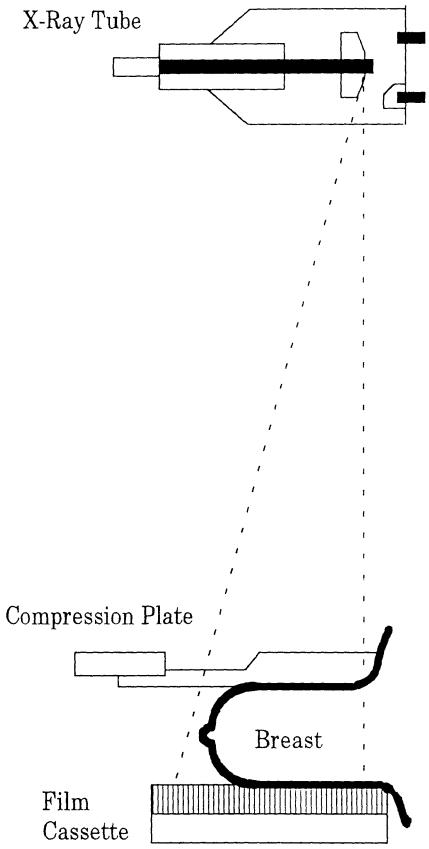

Fig 1.2 *The geometry for the equipment used at mammography examinations. (Adapted from Ref [1].)*

The cost aspect of mass-screening with mammography has been discussed as it is an examination of healthy patients, and as a great part of the cancers are not detected anyway. The money required could instead be used for research on other treatment methods or for more important issues in the public health service. Mammography could then be used just for the women suspected of having cancer or belonging to the risk groups. In most parts of Sweden, however, mass-screening has been accepted as a standard. In Lund a mammography is performed every 18th month for women aged 40 to 74 [7].

Mammography uses ionizing X-ray radiation, so there is always a potential risk of inducing cancer connected to the examination. The risk is greater for young women, and as cancer is more common among elder women, the age of 40 has been chosen for mass-screening. This age is being discussed among experts, and different opinions exist. However 95% of all cancers appear after a woman's 40th year [2]. Several studies show that the mortality in breast cancer decreases by about one third if mass-screening is used for the age group 50 to 69 [1]. For the ages 40 to 49 it is uncertain whether mass-screening lowers the mortality or not, as cancers are difficult to detect in

dense breasts and because there are fewer cancers to be detected in this age group. A risk analysis indicates that the benefit to risk ratio in mass-screening for women aged 35 to 49, is 3.4 to 1 (worst case) [6].

1.3.2 Thermography

In 1957 Lawson demonstrated an increase of IR-radiation from cancerous breasts [8]. Thermography is based on this concept. The elevated heat production is due to a higher metabolism in tumours than in healthy tissue. The heat is transmitted through the tissue to the skin surface, where it can be detected with an IR-sensitive film. A thermal image is generated. No two women have identical thermal prints, but the two breasts should be roughly symmetrical. Obvious asymmetry indicates some kind of abnormality, which is not specific for cancer though. It might also originate from an inflammatory disease. Abnormal thermograms can be seen in about 75% of proven breast cancers [8].

1.3.3 Ultrasonography

In ultrasonography a soundwave is sent into the breast by a transducer. Each surface (i.e. each change in acoustic impedance) in the beam direction will cause an echo. This echo is detected by the transducer, and a sound image is shown on a screen.

Using this method for breasts, was first suggested in the 50's by Wild and Reid, but still has not been thoroughly developed [8]. The technique has difficulties in differentiating between benign and malignant tumours. Solid lesions are irregular in shape and reveal internal echoes and are therefore difficult to see. Another problem is that diagnosis in fatty breasts is difficult, due to differences in acoustic impedance in the fat and in the connective tissue. In dense breasts there is an advantage of ultrasonography over mammography, as the image made is more clearly defined. The method is being used as a complement to mammography today [7].

1.3.4 Magnetic Resonance Imaging

Magnetic Resonance Imaging (MRI) is a method which had its breakthrough at the end of the 70's when Lauterbur made the first successful measurements [6]. The patient is put in a strong magnetic field in order to direct the spins of the atomic nuclei in the body into the same direction. Certain resonance frequencies which alter the spins, are then sent through the body. After turning off these radio frequencies, the atomic spins turn back to their original direction. When doing so, they emit radio signals which can be detected. From these signals it is possible to reconstruct the positions of the nuclei, and an image can be constructed. One advantage with the technique is that it can be used also on women with prostheses. A problem is that a contrast liquid has to be used, in order to being able to distinguish between benign and malignant changes of the tissue. The apparatus used today are large and used for examination of the entire body [1].

1.3.5 Transillumination

Transillumination of the breast by red and near-IR light provides information about both scattering and absorption for different wavelengths in various breast tissues. The mean free path length of a photon in tissue before being scattered is about 100 μm, but each scattering event only causes a small angular deviation on average [9]. This makes it possible to detect light through 3 to 5 cm of breast tissue [10]. Transmitted unscattered light is then negligible. Tumours absorb light stronger than healthy tissue due to the neovascularisation and hereby a higher haemoglobin level. Furthermore, results from other experiments indicate that the scattering in the tumour tissue is decreased due to its cell structure. Further knowledge of the optical properties of tissue is, however, required, before a transillumination technique can be fully developed.

Breast cancer diagnosis by transillumination of the breast with visible light was first discussed by Ewing in 1928 [3]. He did not have much success though, as the method was too uncomfortable for the patient due to heat production of the intense light required. Shortly after Cutler developed a method for water cooling, but the light intensities were still too low to yield a good signal [3].

1.3.5.1 Diaphanography

In the 70's the transillumination technique gained renewed interest as Gros *et al.* developed diaphanography, where a high intensity light source and a recording on photographic film was used [3]. Ohlsson *et al.* improved the method as they started using IR-sensitive film [11]. They suggested that the discrimination between malignant and normal tissue could be that malignant cells contain a higher nitrogen amount than normal connective tissue. Molecules with heavy nitrogen contents have absorption lines derived from vibrations and rotations of the molecules. These absorption lines are mainly in the near-IR region, and the absorption of near-IR light can hence be registered on an IR-sensitive film. This was the concept used by Ohlsson *et al.* [11]. The pendulous breast was illuminated with yellow light, and at this wavelength the light was absorbed to 99.95% on its way through the breast, reemitting red/IR-red light. The breast of a young woman appeared in a red-yellow tone on the IR-film, and the malignant changes appeared in a brown-black colour due to underexposure of the film. The main disadvantages of this method was that the examination was time-consuming and that the examination had to be performed in a dark room.

As mentioned above, light at wavelengths with low absorption must be used in the transillumination technique, otherwise there is too little light left to be detected. Therefore light in the so called "therapeuthic window" between 600 and 1300 nm is mostly used for transillumnination. The dominating attenuation effect in this wavelength region is, however, not the absorption, but the scattering; the scattering coefficient is of the order of 10 cm^{-1}, while the absorption coefficient is of the order of 0.1 cm^{-1} or less [12]. The discrimination between tumours and surrounding tissue can therefore be based on differences in the scattering properties. In order to be sensitive to the scattering properties of the tissue, one would like to observe the light that has interacted only a few times with the tissue. This light has the shortest path through the tissue and hence contains the most spatial information as well. The sensitivity for the absorption properties increases with the path length of the light in the medium, as the

probability for the light to be absorbed increases with path length. However, only a poor spatial resolution can be achieved from such measurements. The poor spatial resolution with the diaphanography method was found to limit its usefulness. At the time when this was found, the idea of using temporally resolved methods was born. Two similar methods have been suggested for this purpose: the time-resolved technique and its equivalent in the Fourier plane - the frequency domain methods. In recent years there has been increasing interest in these techniques.

1.3.5.2 Time-Resolved Methods

In the time-resolved technique the tissue is transilluminated with picosecond laser pulses, and the transmitted light is detected with time-resolution. The light that leaves the tissue first has traveled the straightest and shortest path in the tissue, i.e. it has been less scattered than light exiting later. The early light thus contains more information about the localization of the absorption and scattering centra in the tissue. As tumours scatter light less than normal tissue, the presence of a tumour leads to an increase of the early light. While almost no difference between normal tissue and tumour tissue can be seen in the total transmitted light, the light exiting during the first 120 picoseconds does show a difference. This can be seen in Fig. 1.3. A smaller time-gate gives a better contrast, but it also leads to a lower signal-to-noise ratio, which is illustrated in Fig. 1.4.

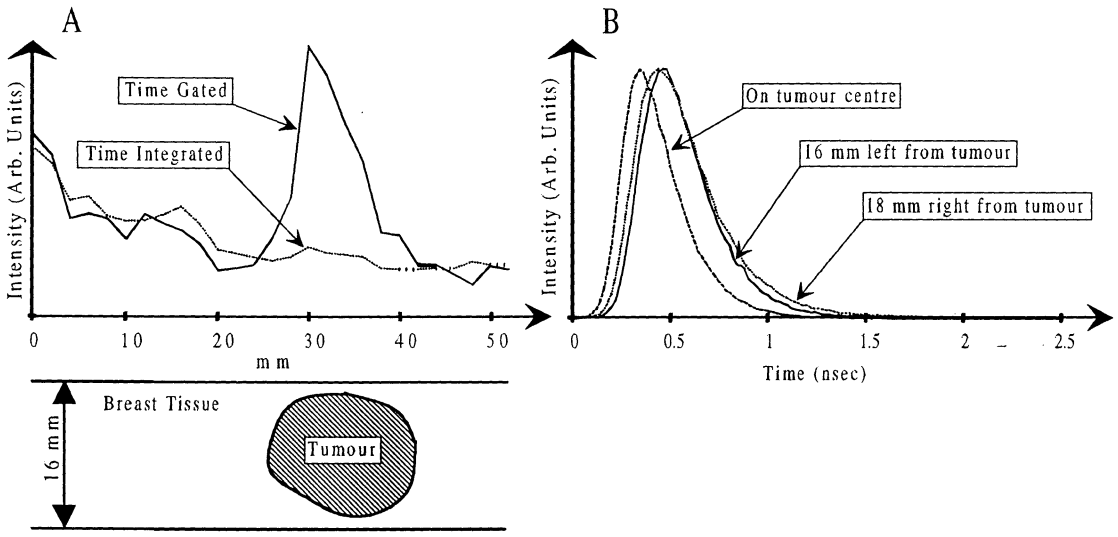

Fig. 1.3 (A) *A scan across a sample of breast tissue 16 mm thick, containing a tumour 18 mm in diameter. The intensity scales for the time-gated and the time-integrated curves are different.*
(B) *The corresponding time dispersion curves for three positions along the scan.*
(From Ref. [10].)

Time-resolved detection can be achieved in several ways. Optical streak cameras, optical Kerr gates or stimulated Raman amplification can be used [13]. These techniques all have high temporal resolution, but relatively high light intensities are

required to obtain a good signal-to-noise ratio with streak camera detectors, and the two other techniques need high power to open their shutters. A more simple technique is to use time-correlated single photon counting, which does not have quite as good temporal resolution, but still gives a high sensitivity [13]. Here the time delay between the laser pulse and a detected photon is measured for a great number of pulses. The probability of detecting more than one photon per laser pulse must be negligible. A time dispersion curve is obtained by constructing a histogram of these time delays.

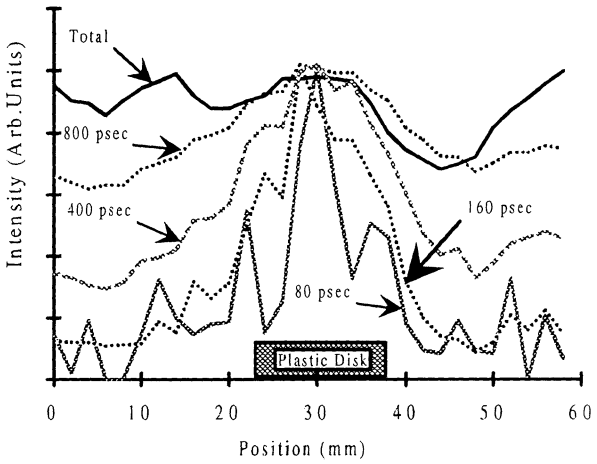

Fig. 1.4. *The contrasts for different time gates when trans-illuminating a 30-mm-thick tissue phantom of animal fat with a plastic disk in the middle. (From Ref. [13].)*

The major disadvantage of this method is that it is very time consuming. The recording time necessary to obtain an acceptable signal-to-noise ratio with a 50 mW laser and a state-of the-art detector is typically 60 seconds per scanning point [10]. If the scanning points are separated by 4 mm, the scanning of a breast takes up to an hour, which of course is much too long.

1.3.5.3 Phase-Resolved Methods

The phase-resolved method is the equivalent of working in the Fourier plane of the time-gated technique. Here the pulsed light source is replaced by an intensity modulated light source, and the phase and intensity modulations are detected instead of the time dispersion curve. The phase shift of the light is a result of the time delay of the photons in the highly scattering medium. Attenuation and time-dispersion of the light due to absorption and scattering cause the demodulation. The equivalent to the demodulation in the time domain representation is the pulse broadening. Some important advantages of the frequency-domain measurements are that the instrumentation can be cheaper and that the acquisition-time might be shortened, due to that better light sources are commercially available [14].

Today there exists several different experimental approaches to perform frequency domain recordings. Most of them originate in fluorescence lifetime measurements. One of them is the cross-correlation detection. The light source can either be a pulsed laser

with picosecond pulses or a sinusoidally modulated laser with modulation frequency ω in the Mega/Giga Hertz range. The gain of the detector is modulated at the frequency $\omega+\Delta\omega$ (heterodyne detection). This is achieved by injecting a radio frequency signal at one of the dynodes of the photo multiplier amplification chain. The gain modulation produces a shift of the high frequency signal detected by the photo multiplier to the convenient low frequency $\Delta\omega$, where accurate digital filtering can be applied. The $\Delta\omega$-signal contains the same information as can be observed directly at the light modulation frequency, and hence the measurements are performed using the $\Delta\omega$ cross correlation signal which is typically below 50 Hz [15, 16]. The two closely spaced frequencies are provided by two frequency synthesizers which are phase-locked to each other.

Another technique uses the concept that the diffusive photon-density waves from two or several light sources can interfere, and that if the sources and detectors are properly configured, this interference permits the localization of an absorbing region in the tissue [17]. Multiple-element source arrays consist of laser diodes modulated 180° out of phase with respect to each other [18]. The diffuse waves which originate from the out-of-phase sources have a null amplitude and a sharp phase transition in the midplane [18]. Chance *et al.* have used a four element linear array with two laser diodes modulated in phase and two modulated out of phase [18, 19]. If an object with different absorbing properties is situated near the midplane of the sources in the sample, a phase-shift can be clearly detected. Patterson *et al.* have used a two-source interference configuration and two detectors. Hence they added signals in interference mode in order to increase the contrast [20]. Presence of multiple objects in the sample decreased the contrast of the interference image, which was a problem. The effects from objects outside the focal region could be decreased, when they used multiple source arrays instead.

1.4 Purpose of this Project

The purpose of this project has been to perform measurements with phase-resolved transillumination equipment. The equipment should be as simple and cheap as possible, and therefore a diode laser was used as light source. The laser was modulated with a sinusoidal signal from a radio frequency generator. The signal was divided into two parts in order to generate a reference signal. The light transmitted through the sample was detected with a photo multiplier tube, whose signal was mixed with the reference signal from the frequency generator. The output from the mixer gave a DC-level proportional to the phase lag of the detected signal after appropriate filtering. Compared with the cross correlation detection system described above, this equipment is much cheaper because only one frequency generator is needed. One drawback is, however, that more noise is picked up by the equipment, as the detection is performed at the same frequency as the modulation of the light source (homodyne detection).

A first step in the project was to examine the signals from the different components of the equipment in order to optimize the signal-to-noise ratio in each step. The detector was built in into a black box, the frequency was optimized and the signal was filtered at this frequency.

After having achieved this first goal, it was time to examine a sample of an Intralipid solution, whose optical properties were similar to those of tissue. By increasing the concentration of the solution, the scattering coefficient of the sample was altered. The phase lag was measured as a function of the concentration of the solution. Finally, tumour phantoms were located in the sample and detected when a scan was made over the entire sample.

2 Light Interaction with Tissue

When illuminating a breast, three types of interaction with the tissue can be observed. Part of the light is reflected, another part is absorbed and the last part is scattered. The probability for each of these interactions to occur is wavelength dependent. This is especially the case for the absorption properties. For one of the major cromophores in tissue - haemoglobin - the absorption cross-section drops two orders of magnitude at about 600 nm. When transilluminating a breast, it is important that as much light as possible can penetrate the tissue, and hence it is important to find a suitable wavelength for the light. In Fig. 2.1 the transmittance for different wavelengths has been investigated *in vivo* for intact nonmalignant human breast. The penetration depth is largest between 650 and 1300 nm - the so called therapeutic window (red and near-IR light). This can be illustrated by putting a lamp emitting white light against the palm of your hand. The light exiting on the other side is no longer white, but red, due to absorption of the shorter wavelengths.

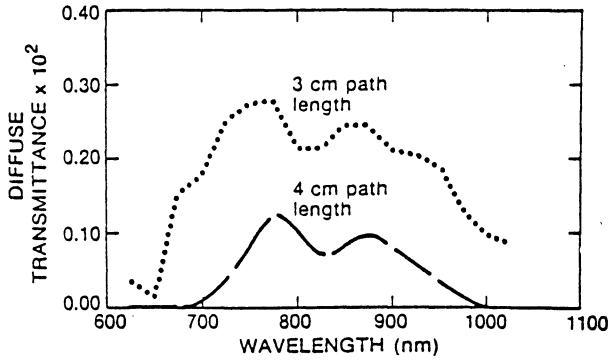

Fig. 2.1. *In vivo measurement of the diffuse transmittance for different wavelengths for intact non malignant human breast. (From Ref. [21].)*

2.1 Reflection

When light passes the interface between two media with different refractive indices, it is partly reflected. The main constituents in breast tissue are water with refractive index 1.33 and fat and proteins with refractive indices of about 1.55. The small-scale heterogeneity of the tissue leads to scattering, while interfaces between two regions of media with a difference in refractive indices can cause a total reflection of about 2-4%, when light passes from air to tissue [22].

2.2 Absorption

Absorption in the tissue is the result of the interaction between the biomolecules and radiant energy. By absorbing light at certain wavelengths, the molecules are either excited to different rotational and vibrational modes or electron transitions occur. The tissue absorbs photons according to Beer's law:

$$I=I_0\exp(-\mu_a L), \quad (1)$$

where μ_a is the absorption coefficient and L is the path length traveled by the photon. The value of L is directly proportional to the time a photon has traveled: L=ct/n, and it is often much longer than the straight path through the tissue, due to multiple scattering [23].

The main absorbers in breast tissue are water, proteins, melanin and haemoglobin [24]. Their absorption can be studied in Fig. 2.2. All proteins absorb strongly in the UV and blue regions, haemoglobin (HbO_2) absorbs in the visible region up to 650 nm and the melanin absorption decreases with wavelength. Water on the other hand absorbs in the IR-region above 1300 nm, which sets an upper limit for useful wavelengths for transillumination diagnostics. There is thus a transmission maxima in the region between 650 and 1300 nm, and this is the wavelength region most useful for transillumination diagnostics. Most work for tissue transillumination has been performed around 800 nm, as detectors and light sources are working best in this region.

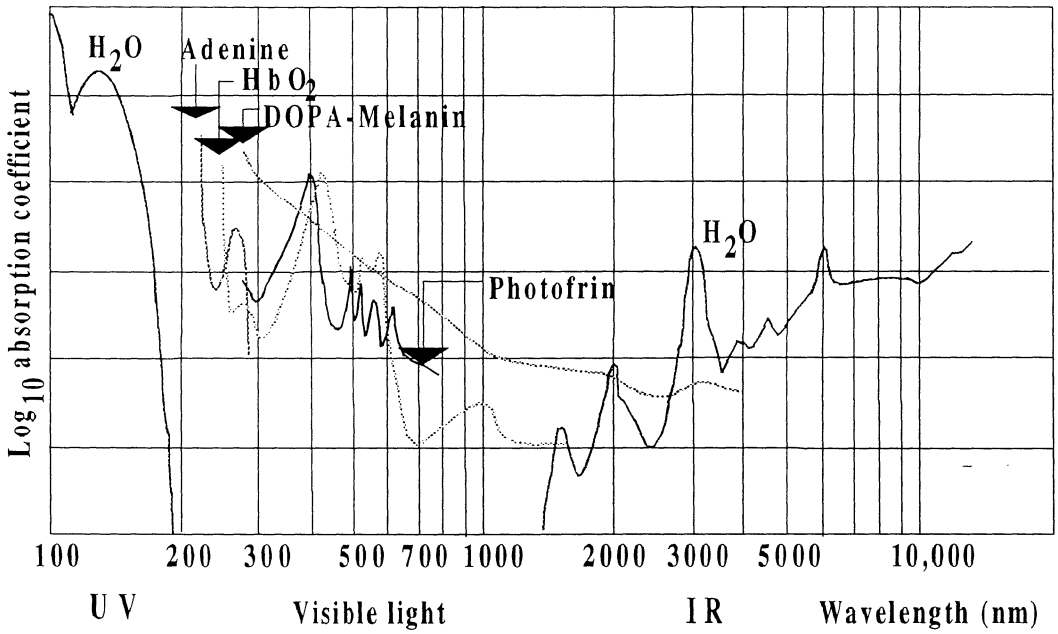

Fig. 2.2. *Absorption curves for a number of tissue constituents. (Adapted from Ref. [24].)*

2.3 Scattering

When using red and near-IR light, the most probable interaction with the tissue is scattering. The mean free path for a photon before being scattered is on the order of 10-100 μm, but the light can still penetrate 30 to 50 mm of tissue [9]. This is mainly due to the fact that most of the scattering events are elastic (i.e. the photon does not

lose any energy) and forward directed [9]. When the scattering particle is smaller than the wavelength, Raman or Rayleigh scattering can occur. Raman scattering is inelastic, whereas Rayleigh scattering is elastic. The scattering probability is proportional to $1/\lambda^4$. If the scattering object on the other hand is larger than the wavelength, Mie scattering occurs. This is an elastic scattering process, with scattering probability proportional to $1/\lambda^2$.

The direction of the scattering is described by the anisotropy parameter $g=\langle\cos\varphi\rangle$, which is the average cosine of the scattering angle. The g-factor is roughly independent of the wavelength, whereas the scattering coefficient slowly falls with increasing wavelength, as can be understood from the inverse wavelength dependency for Mie, Raman and Rayleigh scattering. Within the therapeutic window the g-value is typically 0.8-0.95 for most tissues (Note: cos 37°=0.8; cos 18°=0.95), which represents forward directed scattering [9]. In one picosecond a photon will scatter about 10 times and travel a total distance of about 0.2 mm with 98% probability of not being absorbed [9].

2.4 Theoretical Models

The scattering process makes coherent incident light lose its original direction, and after a very short distance it becomes a diffuse scattered light. The photon transport in the tissue can then be described as a diffusion process, and several models for this process have been made. The exact modeling of light distribution is not possible though, since the tissue is heterogeneous. Assumptions about the optical properties have to be made, and from them a macroscopic light distribution model can be created. Usually coherence effects and inelastic scattering are neglected when making up these models. There are two distinct types of theories dealing with multiple scattering problems: the analytical theory and the transport theory [25]. The theoretical solutions are often confirmed with Monte Carlo computer simulations.

The analytical theory is based on differential equations such as the Maxwell equations or the wave equation. By inserting the absorption and scattering characteristics of the tissue in them, differential or integral equations are obtained. This leads to a rigorous mathematical model including almost all scattering, diffraction and interference effects. In practice it is, however, impossible to solve these equations, as the calculations become to complex.

In the transport theory the wave aspect of the light is neglected and the photons are treated like particles undergoing a large number of collisions instead. All inelastic scattering is also neglected. Even though diffraction and interference effects are included in the scattering and absorption characteristics of a single particle, transport theory itself does not include diffraction effects. Solving the transport equation is the most common method for solving light distribution problems in tissue.

Monte Carlo simulations are often used to confirm theoretical solutions. A point source of photons in a homogeneous lattice with cells having appropriate probabilities for absorption and scattering, can be simulated. A random-number generator samples discrete events from probability distributions derived from the speed of photons in the scattering medium, v, the absorption coefficient, μ_a, the scattering coefficient, μ_s, and

the average cosine of the scattering angle, g. A time histogram can be constructed by simulating a large number of photons, and the light ray can hence be traced on its way through the lattice. The method is conceptually simple, but requires substantial computer resources for precise calculations [26].

2.4.1 The Diffusion Approximation of the Transport Theory

In this paper the transport theory has been used, but it is impossible to solve in its general form, and further approximations have to be made. In highly scattering low-absorbing media the diffusion approximation can be used for the light that has been scattered many times (that means at distances far from the light source (several mean-free path lengths) and a short time after irradiation with a short light pulse). These conditions are fulfilled except for the earliest arriving light, which has not been much scattered. When studying qualitative rather than quantitative phenomena, this approximation can be useful also for the early light used in time-gated transillumination with a gate width of a few hundred picoseconds.

The transport equation is hence simplified to yield the diffusion equation [27]:

$$\frac{\partial}{\partial t}U(\mathbf{r},t)+v\mu_a U(\mathbf{r},t)+\nabla\cdot\mathbf{J}(\mathbf{r},t)=S(\mathbf{r},t), \tag{2a}$$

$$\nabla U(\mathbf{r},t)+\frac{3\partial\mathbf{J}(\mathbf{r},t)}{v^2\partial t}+\frac{\mathbf{J}(\mathbf{r},t)}{vD}=0 \tag{2b}$$

where v is the speed of light in the tissue, $\boldsymbol{r}$ is the source/detector separation, $U(\mathbf{r},t)$ is the density of photons, $\mathbf{J}(\mathbf{r},t)$ is the photon current density, D is the diffusion coefficient, $D=\{3[\mu_a+(1-g)\mu_s]\}^{-1}$ and $S(\mathbf{r},t)$ the photon source. In the case of a sinusoidally intensity-modulated light source, the point source is given by:

$$S(\mathbf{r},t)=\delta(\mathbf{r})F\{1+A\exp[-i(\omega t+\varepsilon)]\} \tag{3}$$

where $\delta(\mathbf{r})$ is a Dirac delta function located at the origin, F is the fluence of the source (in photons per second), A is the modulation of the source, ω is the angular modulation frequency of the source and ε is an arbitrary phase.

For a homogenous infinite medium Fishkin *et al.* have found an analytical solution to Eqs (2) in the frequency domain under the assumptions that the modulation frequency is much smaller than the typical frequency of the scattering process (i.e. $\omega<<v\mu_s(1-g)$, where v is the speed of light in the medium) [27]. When substituting Eq. (3) into Eq. (2a) and assuming that $U(\mathbf{r},t)$ and $\mathbf{J}(\mathbf{r},t)$ are on the forms:

$$U(\mathbf{r},t)=[U(\mathbf{r})]_{dc}+[U(\mathbf{r})]_{ac}\exp[-i(\omega t+\varepsilon)], \tag{4a}$$

$$\mathbf{J}(\mathbf{r},t)=[\mathbf{J}(\mathbf{r})]_{dc}+[\mathbf{J}(\mathbf{r})]_{ac}\exp[-i(\omega t+\varepsilon)], \tag{4b}$$

the steady state equations (i.e. the DC-part):

$$v\mu_a[U(\mathbf{r})]_{dc} + \nabla\cdot[\mathbf{J}(\mathbf{r})]_{dc} = F\delta(\mathbf{r}), \tag{5a}$$

$$[\mathbf{J}(\mathbf{r})]_{dc} = -vD\nabla[U(\mathbf{r})]_{dc} \tag{5b}$$

and the frequency-dependent equations (i.e. the AC-part):

$$(v\mu_a - i\omega)[U(\mathbf{r})]_{ac} + \nabla\cdot[\mathbf{J}(\mathbf{r})]_{ac} = FA\delta(\mathbf{r}), \tag{6a}$$

$$[\mathbf{J}(\mathbf{r})]_{ac} = -vD\left[\frac{1+i3\omega D/v}{1+(3\omega D/v)^2}\right]\nabla[U(\mathbf{r})]_{ac} \tag{6b}$$

are obtained. The assumption that $\omega D << v$, reduces Eq. (6b) to:

$$[\mathbf{J}(\mathbf{r})]_{ac} \cong -vD\nabla[U(\mathbf{r})]_{ac}. \tag{7}$$

The variable $[\mathbf{J}(\mathbf{r})]_{ac}$ can be eliminated from Eqs (5). The steady-state diffusion equation:

$$\nabla^2[U(\mathbf{r})]_{dc} - (\mu_a/D)[U(\mathbf{r})]_{dc} = -F/(vD)\delta(\mathbf{r}) \tag{8}$$

is then obtained. The variable $[\mathbf{J}(\mathbf{r})]_{ac}$ can be eliminated from Eq. (6a) by expression (7). This gives the frequency-dependent diffusion equation:

$$\nabla^2[U(\mathbf{r})]_{ac} - \left(\frac{v\mu_a - i\omega}{vD}\right)[U(\mathbf{r})]_{ac} = -\frac{FA}{vD}\delta(r). \tag{9}$$

For an infinite medium Eqs (8) and (9) can be solved to yield:

$$U(\mathbf{r},t) = \frac{F}{4\pi vDr}\exp\left[-r\left(\frac{\mu_a}{D}\right)^{1/2}\right] + \frac{FA}{4\pi vDr}$$
$$\times\exp\left\{-r\left(\frac{v^2\mu_a^2+\omega^2}{v^2D^2}\right)^{1/4}\cos\left[\frac{1}{2}\arctan\left(\frac{\omega}{v\mu_a}\right)\right]\right\}$$
$$\times\exp\left\{ir\left(\frac{v^2\mu_a^2+\omega^2}{v^2D^2}\right)^{1/4}\sin\left[\frac{1}{2}\arctan\left(\frac{\omega}{v\mu_a}\right)\right] - i(\omega t+\varepsilon)\right\}. \tag{10}$$

For a nonabsorbing medium, i.e. μ_a=0, Eq. (4) reduces to:

$$U(\mathbf{r},t) = \frac{F}{4\pi vDr} + \frac{FA}{4\pi vDr}\exp\left[-r\left(\frac{\omega}{2vD}\right)^{1/2}\right]\times\exp\left[ir\left(\frac{\omega}{2vD}\right)^{1/2} - i(\omega t+\varepsilon)\right].$$

(11)

Examination of Eq. (11) shows that $U(\mathbf{r},t)$ constitutes a scalar field which is propagating at a constant speed in a spherical wave, and attenuates as $\exp(-\alpha r)/r$ as it propagates. The second exponential term represents the phase of the wave.

It can also be seen that the photon density wave emitted from a source with modulation frequency ω, has a wavelength of:

$$\lambda = 2\pi\sqrt{2vD/\omega} \tag{12}$$

and that its wave front advances at constant speed:

$$V=\sqrt{2vD\omega} \quad . \tag{13}$$

Note that Eqs (12) and (13), respectively, describe the wavelength and phase velocity of a photon density wave, and not the colour and velocity of the light itself.

Eq. (10) is the Fourier transform equivalent of:

$$U(\mathbf{r},t) = \frac{1}{(4\pi vDt)^{3/2}} \exp\left(-\frac{r^2}{4vDt} - \mu_a vt\right), \tag{14}$$

which is the time-dependent solution of the diffusion equation as reported by Patterson *et al.* [28]. Here the photon source term is a narrow pulse given by $S(\boldsymbol{r},t)=\delta(\boldsymbol{r})\delta(t)$. There is a practical difference in describing photon diffusion in the frequency domain with respect to its Fourier transform equivalent in the time domain; the photon density wave generated by a sinusoidally modulated source propagates coherently, while pulses do not. This fact is schematically described in Fig. 2.3. In the figure it can be seen how a pulse is broadened when traversing a highly scattering medium due to the distribution of optical paths taken by the photons arriving to the detector. If, on the other hand, the light source is sinusoidally modulated, the transmitted wave will remain modulated with the same frequency as the incoming wave as can be seen in Fig. 2.3.b. The transmitted wave is however delayed due to a lower phase velocity in the medium, and the amplitude is reduced due to scattering and absorption.

The quantities that are measured in a frequency domain experiment are the phase lag of the signal at the detector relative to the one at the source, the average intensity of the detected signal (i.e. the DC-level) and the amplitude of the frequency dependent part of the detected signal (i.e. the AC-level) as shown in the figure. Eq. (10) yields expressions for these quantities:

$$\Phi = r\left(\frac{v^2\mu_a^2+\omega^2}{v^2D^2}\right)^{1/4} \sin\left[\frac{1}{2}\arctan\left(\frac{\omega}{v\mu_a}\right)\right] \tag{15}$$

$$\ln[(r)(DC)] = -r\left(\frac{\mu_a}{D}\right)^{1/2} + \ln\left(\frac{F}{4\pi vD}\right) \tag{16}$$

$$\ln[(r)(AC)] = -r\left(\frac{v^2\mu_a{}^2 + \omega^2}{v^2D^2}\right)^{1/4} \times \cos\left[\frac{1}{2}\arctan\left(\frac{\omega}{v\mu_a}\right)\right] + \left(\frac{FA}{4\pi vD}\right) \qquad (17)$$

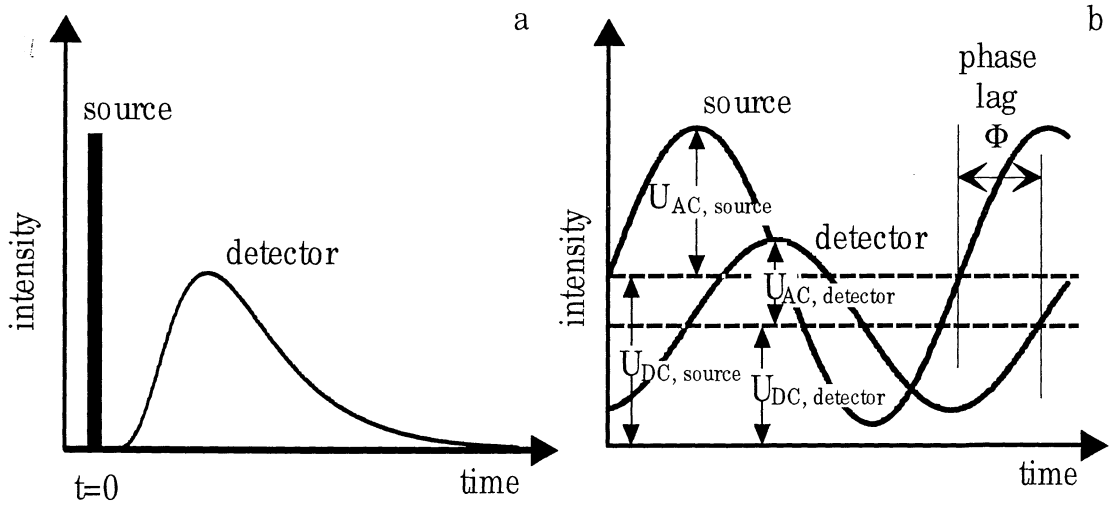

Fig. 2.3. (a) *Schematic representation of the time evolution of the light intensity measured in response to a narrow light pulse traversing a scattering and absorbing medium. The broadening of the pulse arises from the fact that different paths are taken by the photons due to scattering.*
(b) *The time evolution of the intensity measured when a wave from a sinusoidally intensity-modulated source traverses the same medium. The transmitted wave retains the same frequency as the incoming wave, but is delayed due to a lower phase velocity in the medium. The demodulation arises from attenuation related to scattering and absorption of photons. This is the equivalent of the pulse broadening in (a).*
(From Ref. [29].)

The above three expressions are all linear functions of the source/detector separation r, but have a more complicated dependency on ω, v, μ_a, μ_s and g. Thus it can be seen that the linear dependency of $\ln[(r)(AC)]$, $\ln[(r)(DC)]$ and Φ on r is a necessary, but not sufficient condition for the validity of the diffusion approximation of the Boltzmann transport equation.

3 Materials and Methods

Two experimental setups were used. First a mode-locked argon-ion dye laser was used as light source, and the frequency components of the detected signal were studied by Fourier transformation. This was done in order to demonstrate the equivalence of the time-resolved and the frequency-resolved methods, and to see if the equipment used was suitable for this kind of measurement. Another purpose of the experiment was to study the characteristics of the PMT.

In the next experiment, the light source was a sinusoidally intensity modulated diode laser. The same detector as in the first experiment was used. In this experiment light transmitted through a sample whose scattering characteristics were altered during the experiment was detected. The results from these experiments were confirmed with computer simulations.

3.1 Mode-Locked Dye Laser Setup

Fig. 3.1 shows the setup for the first experiment. The light source was a mode-locked Coherent Innova Argon-ion laser pumping a Coherent CR 599-04 dye laser equipped with a Coherent 7210 cavity dumper. The dye used was Rhodamin 6G. The pulses from the dye laser were measured to be 4.4 ps with an auto correlator, and the repetition rate was 76 MHz. The average output power was about 50 mW at the chosen wavelength of 630 nm.

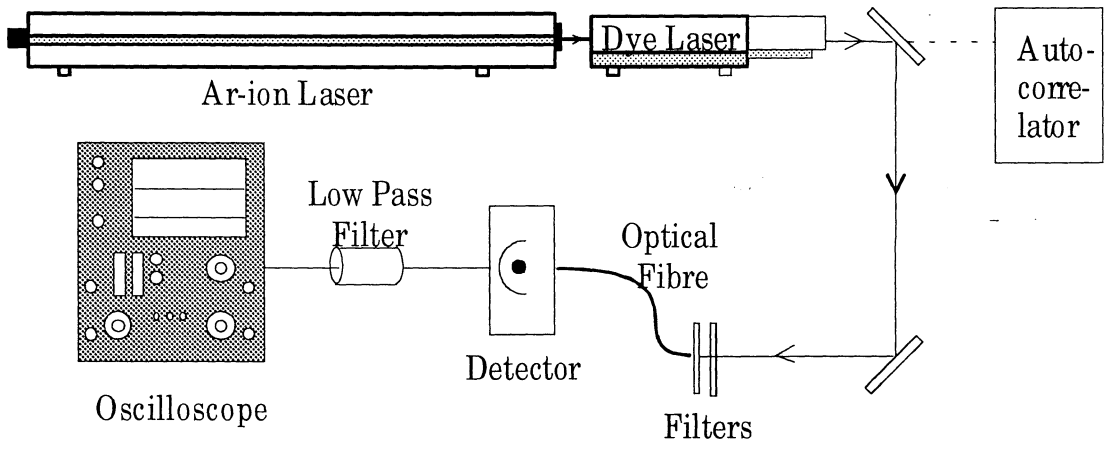

Fig. 3.1. *Setup for the mode-locked dye laser experiment*

The light was guided via a fibre through different neutral density filters and to the detector. The filters were there in order to make it possible to change the amount of light reaching the detector and hence vary its gain.

Two kinds of detectors were used: first a photo diode and then a photo multiplier tube, Hamamatsu R928. The signal from the PMT was studied at different light intensities

and PMT gains. At low light intensities, the PMT gain had to be kept high. The light entering the PMT then gave rise to electron bursts, which were seen on the digital oscilloscope (Tektronix TDS 520A). In this high-gain mode the modulation signal was difficult to identify. However, when connecting two band pass filters (76 MHz) and one low pass filter (100 MHz), and then Fourier transforming the signal, the frequency components of the detected signal could be studied.

3.2 Diode Laser Setup

The experimental setup for phase-resolved transillumination is shown in Fig. 3.2. A radio frequency generator (General Radio Company 1364-B) modulated a laser diode at the frequency 65 MHz. This frequency was chosen after varying the frequency between 50 MHz and 250 MHz. At 65 MHz the disturbing signals picked up by the surrounding equipment, were smaller than at other frequencies.

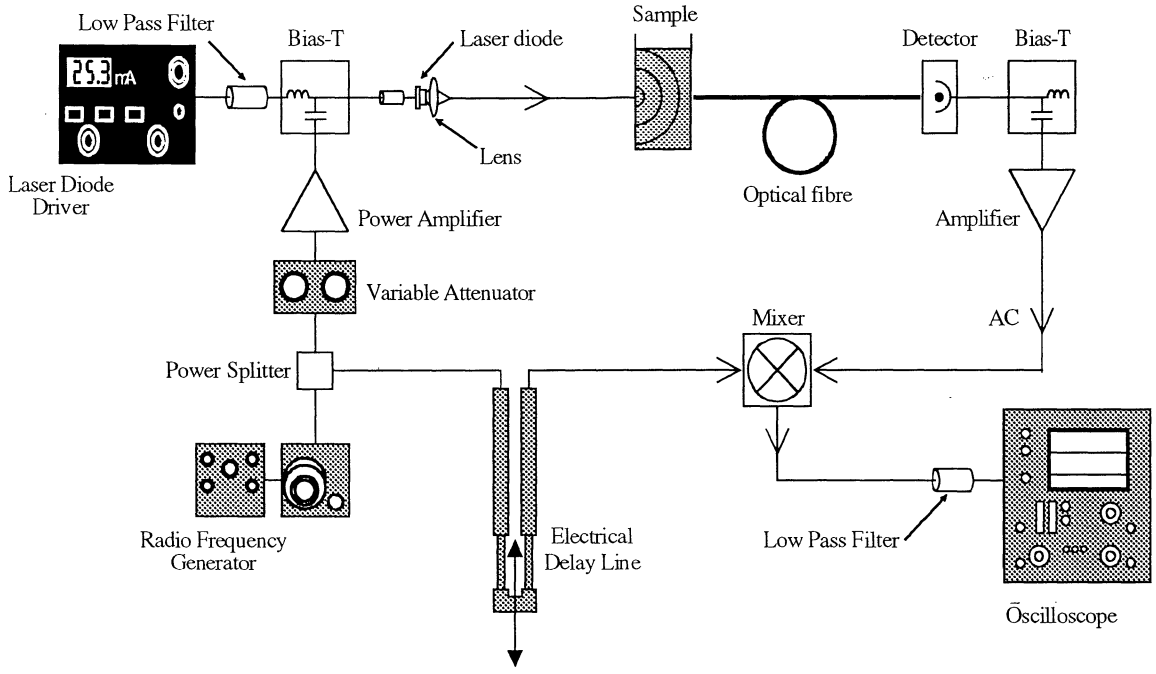

Fig 3.2. *Setup for diode laser experiment*

The signal from the oscillator was divided into two halves by a power splitter. The first half of it was used as a reference signal in the mixer, whereas the other was fed together with a DC-signal to the laser diode. The modulated laser beam was focused onto the sample, and then collected by an optical fibre, after passing through the sample. The fibre guided the light to the PMT (the same as used in the experiment mentioned above), where the light signal was transformed into an electrical current signal. This signal was amplified, and then mixed with the reference signal in a mixer. The output signal from the mixer was proportional to the cosine of the phase difference between the reference signal and the detected signal.

In this experiment the phase difference between the reference signal from the radio frequency generator and the signal from the PMT was studied. The phase of the reference signal could be altered by changing the path length through the electrical delay line. The phase of the detected signal increased, when the scattering coefficient in the sample was raised.

3.2.1 The Laser

The light source in this experiment was a SHARP laser diode (LT024MDO, 30 mW) emitting near-IR light with a wavelength of 790 nm. The four main reasons for using this laser were as follows:

- It produces light in the near infrared region, where tissue is most transparent.
- It is small, easy to handle and relatively inexpensive.
- It is easily modulated with a radio frequency generator.
- It emits light below 800 nm, where the detector still has a good sensitivity.

3.2.2 The Sample

The scattering and absorption properties of the sample should be similar to those of breast tissue. Therefore a liquid called Intralipid 200 mg/ml (Kabi Vitrum, Stockholm) was chosen. Intralipid is a fat emulsion which is clinically used as an intravenously administered nutrient. It consists of glycerin, lecithin, soybean oil and water, and looks like milk. The scattering particles consist of soybean oil encapsulated in lecithin, and they are approximately spherical [30]. The absorption coefficient is low in comparison to the scattering coefficient, just like in tissue. In healthy breast tissue the scattering coefficient is about 10 cm^{-1}. In the Intralipid solution the scattering coefficient was 3.9 cm^{-1}/[g/l] Intralipid (as measured in a narrow beam experiment, see Fig. 3.3).

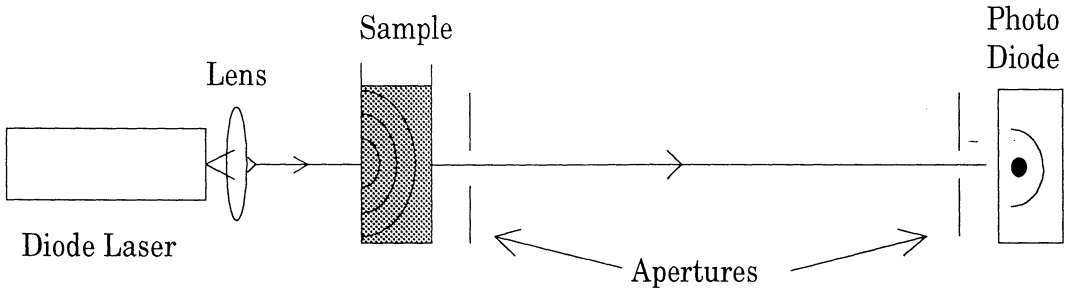

Fig. 3.3. *Experimental setup for a narrow beam experiment. The Intralipid solution was added ml by ml to the cuvette. Only the forward scattered light reached the detector, and in this way the scattering coefficient of the solution could be measured to be 3.93 cm^{-1}/[g/l].*

A glass cuvette with the dimensions 95 x 95 x 30 mm was filled with 200 ml water. The laser beam was focused onto the center of the cuvette side, to avoid unwanted diffraction effects at the borders of the sample. An optical fibre collected the exiting light on the other side of the cuvette, and led it to the PMT. Then an Intralipid solution with concentration 10 mg/ml was added ml by ml. In this way the optical properties of

the solution were easily altered and the relationship between the phase shift and the scattering coefficient could be studied. The scattering coefficient was varied from 1.8 cm^{-1} to 9 cm^{-1}.

In a second experiment the concentration of the liquid was kept at a high and constant level (μ_s=9.1 cm^{-1}). Two transparent glass rods with different diameters (15 mm and 8 mm respectively) were placed in the center of the cuvette, and a scan was made over the cuvette side, to see whether they gave rise to a phase shift or not. Then a black plastic rod (with diameter 7 mm) was used, in order to see what happened when a local absorber was present.

3.2.3 The Detector

The PMT used, Hamamatsu R928, was the same as in the mode-locked dye laser experiment. It was built in into a black box to minimize the radio-frequency pick-up in the connecting cables. The box only has two inputs: one hole for the optical fibre and one for a 220 volt AC cable, and one output: a coaxial cable with the amplified signal. Inside the box there is a socket containing a high voltage generator which was biased with a DC that can be varied with a potentiometer. In this way the high voltage could be continuously changed between 0 and 1000 volts. At the voltage 1000 volts the amplification of the PMT was 1×10^7.

3.2.4 The Mixer

The mixer is an electronic component which multiplies two signals. If the two signals are on the form:

$$U_1=A\sin(\omega_1 t+\varepsilon_1) \text{ and } U_2=B\sin(\omega_2 t+\varepsilon_2), \tag{18}$$

with angular frequencies ω_1 and ω_2 and phases ε_1 and ε_2, an ideal mixer will multiply them and give the result:

$$U=U_1U_2=A\sin(\omega_1 t+\varepsilon_1)B\sin(\omega_2 t+\varepsilon_2). \tag{19}$$

This can also be written as:

$$U=\frac{AB}{2}\{\cos((\omega_1-\omega_2)t+\varepsilon_1-\varepsilon_2)-\cos((\omega_1+\omega_2)t+\varepsilon_1+\varepsilon_2)\}. \tag{20}$$

In this experiment the two signals had the same frequency ($\omega_1=\omega_2=\omega$), as they both originated from the same radio frequency generator. Since only the relationship between the two phases was important, ε may be substituted for ε_1 and 0 for ε_2. Eq. (19) then reduces to:

$$U=-\frac{AB}{2}\{\cos(2\omega t+\varepsilon)-\cos(\varepsilon)\}. \tag{21}$$

When this signal was low pass filtered, the remaining signal was a DC-level ($U=\frac{AB}{2}\cos\varepsilon$) only depending on the amplitudes and the phase difference between the two mixed signals.

3.3 Numerical Predictions

The results from the experiments with the rods were compared with results from numerical computer calculations. The relationship between the demodulation and the phase shift of the signal was calculated as a function of the modulation frequency.

The program used for these simulations has been developed at the Division of Atomic Physics at Lund Institute of Technology [31]. The program simulates light diffusion through a slab of tissue, described by a three-dimensional matrix. For a homogeneous tissue slab with slab thickness d and infinite length the diffusion equation (Eq. 14) has been solved by Patterson *et al.*:

$$U(d,t)=(4\pi Dv)^{-1/2}t^{-3/2}\exp(-\mu_a vt)\times\{(d-z_0)\exp\left[-\frac{(d-z_0)^2}{4Dvt}\right]$$
$$-(d+z_0)\exp\left[-\frac{(d+z_0)^2}{4Dvt}\right]+(3d-z_0)\exp\left[-\frac{(3d-z_0)^2}{4Dvt}\right]$$
$$-(3d+z_0)\exp\left[-\frac{(3d+z_0)^2}{4Dvt}\right]\} \qquad (22)$$

where $z_0=\left[(1-g)\mu_s\right]^{-1}$.

In the program the diffusion equation is translated into a differential equation with finite steps in the x, y, z and time variables. Then a tridiagonal system of equations is yielded. The computer uses a generalized Crank-Nicholson algorithm in three dimensions for solving this system. The algorithm is called the ADI (Alternating Direction Implicit) method, and it solves the equations for the three dimensions separately by using one third of each time-step for the x, y and z variables respectively. The resulting equation for the x dimension is:

$$U_{xyz}^{t+1/3}-U_{xyz}^{t}=\frac{c\Delta t}{3n\Delta^2}\{D_{x+1/2yz}\left(U_{x+yz}^{t+1/3}-U_{xyz}^{t+1/3}\right)-D_{x-1/2yz}\left(U_{xyz}^{t+1/3}-U_{x-yz}^{t+1/3}\right)$$
$$+D_{xy+1/2z}\left(U_{xy+z}^{t}-U_{xyz}^{t}\right)-D_{xy-1/2z}\left(U_{xyz}^{t}-U_{xy-z}^{t}\right)$$
$$+D_{xyz+1/2}\left(U_{xyz+1}^{t}-U_{xyz}^{t}\right)-D_{xyz-1/2}\left(U_{xyz}^{t}-U_{xyz-1}^{t}\right)\}$$
$$-\frac{c\Delta t}{6n}\mu_a\left(U_{xyz}^{t}-U_{xyz}^{t+1/3}\right) \qquad (23)$$

where U^{t}_{xyz} is the fluence rate in the matrix element (x, y, z) at time t, Δt is the time step, Δ is the step size in the x, y and z directions and $D_{x+1/2yz}$ is the average of the diffusion coefficient in the matrix elements (x, y, z) and (x+1, y, z) [31].

The light source is represented as a picosecond light pulse that incidents normally at the center of one of the sides of the sample, and the exiting light was then detected on the other side, just as in the laboratory experiment. The resulting time dispersion curve was Fourier transformed to move from the time plane to the frequency plane.

The black rod was represented by a cylindrical area of high light absorption and with the same scattering properties as in the surrounding medium. The glass rod had the same absorption as the medium, whereas 10% of the scattering coefficient of the surrounding medium was used as its scattering coefficient.

4 Results

4.1 Mode-Locked Dye Laser Experiment

In this experiment two kinds of detectors, a photo diode and a PMT, were studied at different light intensities. At high light intensities, the photo diode gave the best signals as it did not pick up disturbing signals from the surroundings to the same extent as the PMT. At low light intensities, however, it was not sensitive enough to give an acceptable signal-to-noise ratio. Therefore it was clear that a PMT had to be used in the further experiments.

The signal-to-noise ratio was optimised for high light intensities, by reducing the gain of the PMT. The scattered light, studied in the next experiment, gave a very weak signal, meaning that the gain had to be kept high in all realistic experiments. The light entering the PMT then gave rise to electron bursts, which were seen on the oscilloscope. This photon counting mode made it hard to evaluate the modulated signal. In Fig. 4.1 the signal (a) and its Fourier transform (b) can be seen. In this recording a medium light intensity and PMT gain were used. From this signal it is difficult to directly extract any useful information, but after connecting two band pass filters (76 MHz) and one low pass filter (100 MHz), and then Fourier transforming the signal, the frequency component of 76 MHz from the incoming signal, could be clearly detected. See Fig. 4.2.a and 4.2.b.

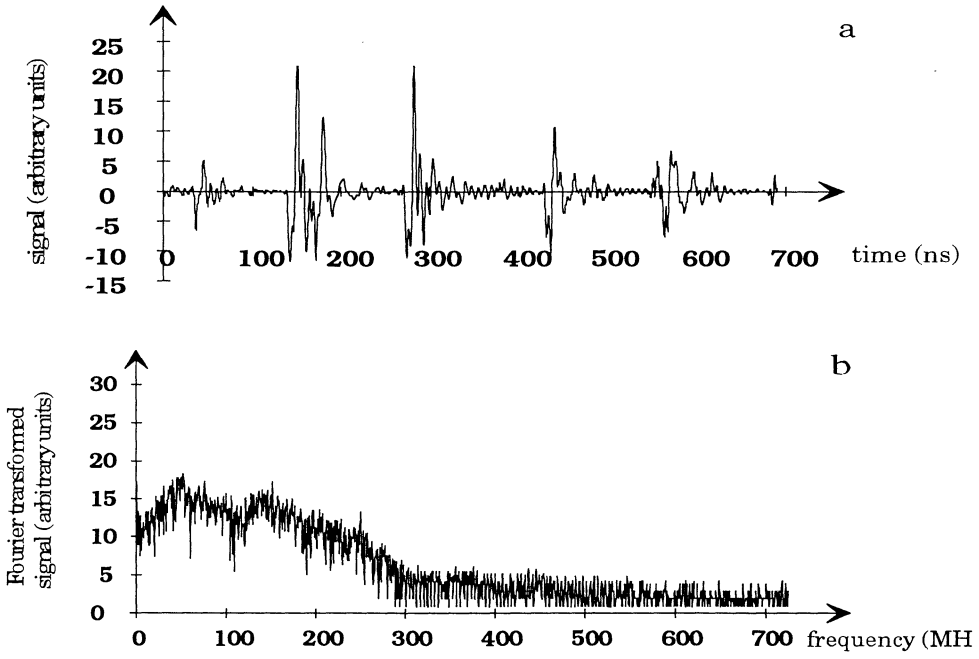

Fig 4.1. *The signal from a pulsed picosecond laser, as detected by a photo multiplier tube (a), and its Fourier transform (b).*

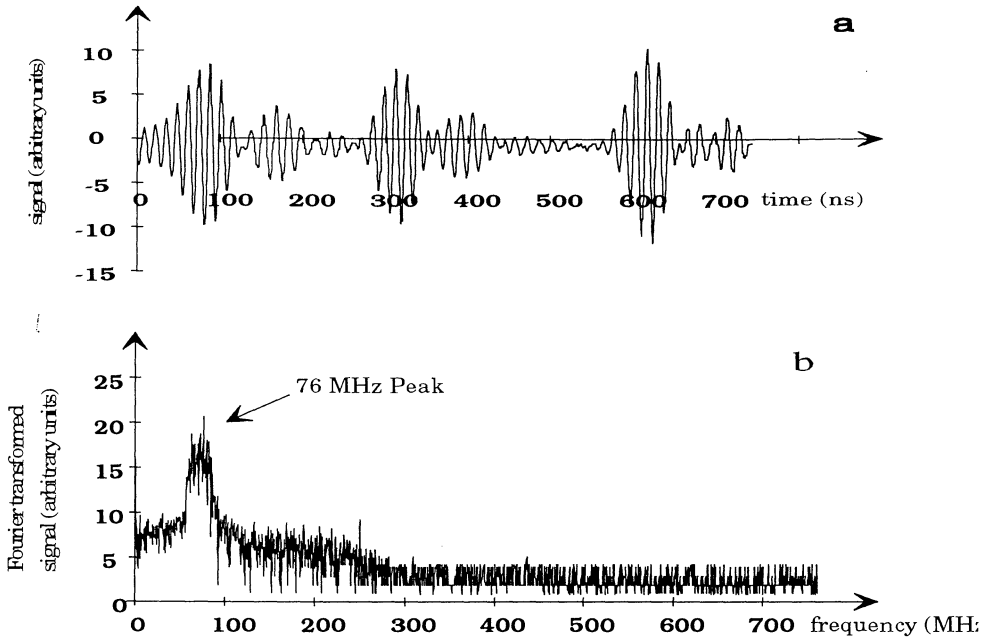

Fig. 4.2. *A similar signal as in Fig. 4.1.a after filtering with a low pass filter(100 MHz) and with two band pass filters (76 MHz) (a) and its Fourier transform (b).*

Thus it was proven that this setup could have been used for further experiments. The aim of these experiments had, however, been to increase the understanding of the different components in the setup, and to show the equivalence between time-resolved and frequency-resolved measurements. Next step was to reduce the cost and complexity of the equipment, and therefore a sinusoidally modulated diode laser was used as light source.

4.2 Diode Laser Experiment

In the first real measurements the relationship between the phase and the concentration of the Intralipid solution was studied. The cuvette was filled with 200 ml of water. The reference signal and the detected signal were phase matched with the electrical delay line, which could be seen as a maximum signal from the mixer. Then the Intralipid solution (with concentration 10 mg/ml) was added ml by ml. At each measuring point the maximum signal (phase=0°), the minimum signal (phase=180°) and the signal at a certain length of the electrical delay line was studied. The relationship between these signals gave the phase of the signal at each concentration of Intralipid. In Fig. 4.3 the logarithm of the phase, Φ, is plotted versus the logarithm of the concentration of the solution, c, which in turn is proportional to the scattering coefficient, μ_s. According to theory, the phase should follow formula (15) (see page 22), which for a non absorbing medium reduces to:

$$\Phi = r\left(\frac{3\omega(1-g)\mu_s}{2v}\right)^{1/2} \tag{24}$$

where v is the speed of light in the sample, $v=\frac{c}{n}\approx\frac{c}{1.4}$ m/s, ω is the angular frequency, $\omega=2\pi f=2\pi 65*10^6$ rad/s, r is the light source/detector separation, r=3 cm, and $(1-g)\mu_s$ is the reduced scattering coefficient. As previously mentioned the scattering coefficient was measured to be 3.93 cm^{-1}/[g/l], and after curve fitting with all known parameters a g-value of 0.84, 0.87 and 0.92, in measurement a, b and c respectively, was calculated. This value is somewhat higher than the expected value of 0.7-0.8 [10].

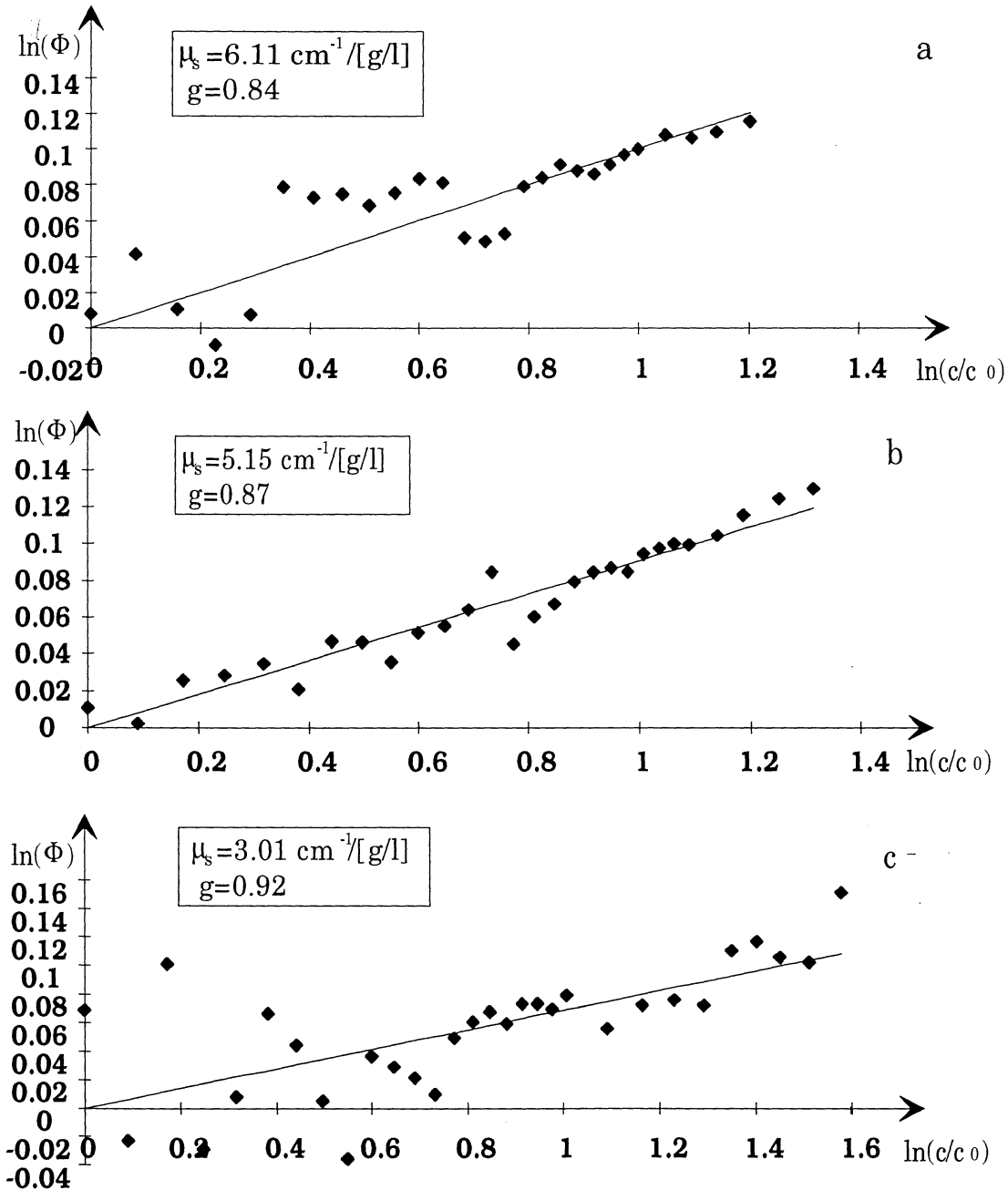

Fig 4.3. *Three measurements of the relationship between the phase shift of the signal (Φ) and the concentration (c) of the Intralipid solution in mg/ml (logarithmic plot). The μ_s- and g-values are calculated from formula (24) after curve fitting with known parameters.*

In the experiments with glass rods, a phase shift could be seen as expected. The light now had a shorter path through the sample, and hence the phase lag between the reference signal and the detected signal decreased. The diameters of the rods were 15 and 8 mm, and the phase as a function of the x-coordinate for the rods can be seen in Figs. 4.4.a and 4.4.b.

The black plastic rod also gave rise to a detectable phase shift. This shift was in the same direction but relatively larger than in the glass rods, as can be seen in Fig. 4.4.c.

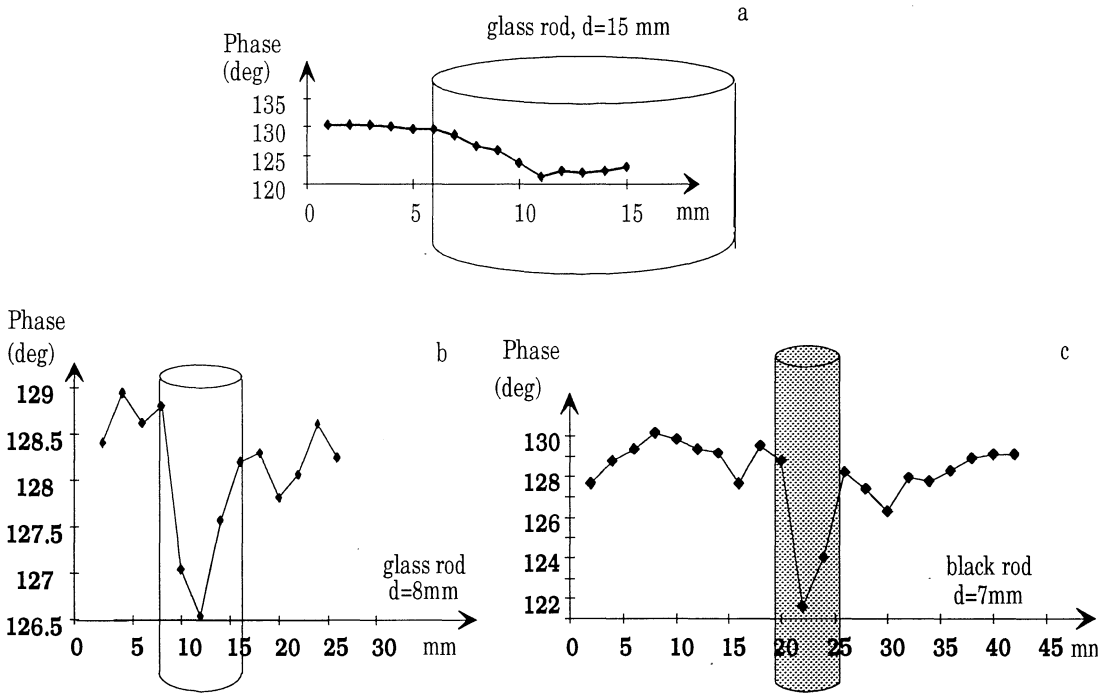

Fig. 4.4. *The phase shift of the signal was measured, when a scan was made over the cuvette side. The cuvette contained an Intralipid solution with concentration 2.3 mg/ml* (μ*=9.1 cm*$^{-1}$*) and a glass rod (Figs a and b) or an absorbing rod (Fig. c).*

4.3 Numerical Calculations

Computer simulations were made for comparison to the experimental results from the rod experiments (see above). The dependency of the demodulation (Fig. 4.5.a) and the phase shift (Fig. 4.5.b) of the signal to its frequency was studied as well. In Fig. 4.5.c the phase difference, due to presence of either an absorber or a glass rod inside a highly scattering medium, is presented as a function of the modulation frequency. It is worth pointing out that the absorber gives rise to a higher phase shift than the scatterer up to 1 GHz and then decreases until it eventually becomes negative at even higher frequencies (not presented here). The phase shift due to the glass rod increases with the frequency up till 1.2 GHz, then the curve starts to show oscillations. These must come

calculations confirmed the direction of the phase shifts and also the fact that the absorber gave rise to a higher shift than the glass rod (see Fig. 4.5.c).

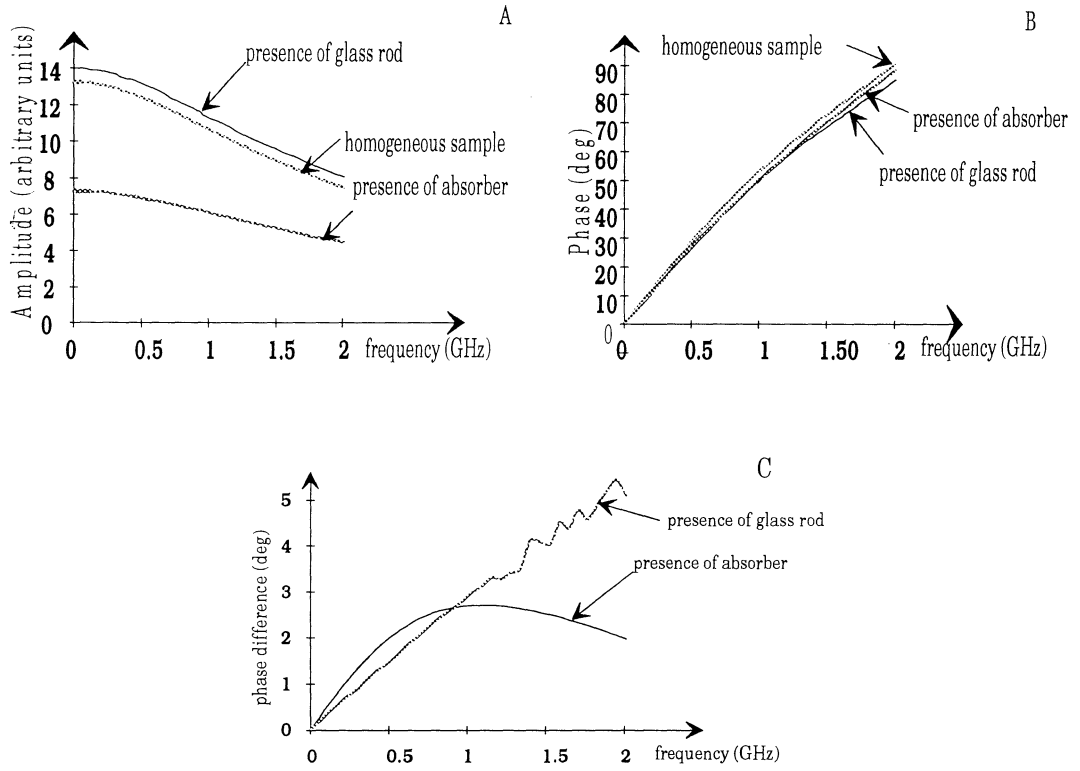

Fig. 4.5. *Computer simulations of the dependency between demodulation (A) and phase shift (B) of a signal and its frequency were performed for three tissue phantoms: one homogenous medium, one highly scattering medium containing a cylindrical absorber and another containing a glass rod. In Fig. C the difference between the phase shift in the homogenous phantom and in the absorber or glass rod containing medium, is presented as a function of the frequency.*

5 Discussion and Conclusions

5.1 Discussion

The aim of this project has been to investigate a phase-resolved transillumination method designed to detecting early stage breast tumours. The main purpose was to become more familiar with the method itself, and to examine the different components of one possible experimental setup. The simplest possible setup was chosen. Therefore, homodyne detection was used, which, to our knowledge, has not been investigated for this purpose by other groups. The homodyne detection lowers the costs considerably compared with the most frequently used technique, the cross-correlation method, as only one radio frequency generator is needed. Another way of lowering the costs was to use a diode laser, instead of larger more expensive lasers, as a light source.

There has, however, been several problems to struggle with during the experiments, and the chosen setup was perhaps too simple. The main problem was to get rid of disturbing signals picked up from the surroundings. The diode laser used did not have enough power for measurements in realistically thick samples. The signal reaching the PMT was therefore very weak, which meant that the highest amplification possible in the PMT had to be used. In the high amplification mode the shot-noise gets increasingly important, which led to an unstable signal. As only one frequency generator was used for both the laser modulation and for the reference signal, noise picked up by the components in the equipment from the frequency generator, strongly affected the measurements. This meant that the frequency giving rise to the smallest possible noise had to be chosen for the measurements. At the highest frequencies, the noise, picked up in the amplifier after the PMT, was so strong that no useful signal could be detected. This was, however, possible at lower frequencies. It was, on the other hand, desirable to use the highest possible frequency, as the detected phase shift increases with frequency.

The signal-to-noise ratio was optimised at 65 MHz. Here a phase shift could be detected, when changing the scattering properties of the tissue phantom. The problem was that the shift at such a low frequency is very small, which made it hard to obtain consistent results between two sequential measurements of the same object as can be seen in Fig. 4.3. This problem was most severe when glass rods and absorbing rods were placed in the highly scattering medium. A shift in the expected direction could always be seen, but the magnitude varied considerably.

Finally some numerical calculations were made with a computer program, in order to compare the experimental results with theoretical predictions and to give an increased understanding of the frequency dependency of the phase shift. The calculations confirmed some trends seen in the experiments, and they also made clear that it would have been wiser to work at higher frequencies. Firstly, it was confirmed that an absorber gives rise to a larger phase shift than a glass rod at low frequencies. Secondly, it was made clear that both a glass rod and an absorber give rise to negative phase shifts at low frequencies. In the case of the glass rod this seems reasonable, as the light is not scattered in the glass and hence is allowed to take a shorter way through the sample. For the absorber, however, the relationship was more complicated. The intuitive guess would be that when the light passes through a sample with an absorbing

rod in it, it should be forced to take a longer path around the rod in order to reach the detector. This should lead to a positive phase shift, which is what can be seen at high frequencies. At low frequencies, however, the phase shift is negative. This can be understood by considering the long path length the light at these low frequencies will have in the medium. It is likely that the photons, in passing the medium, sooner or later will reach the absorber. One can thus instead imagine a sample with a homogeneous distribution of small absorbers, instead of one big absorber in the middle of the sample. The photons that take a long path through such a medium are obviously more likely to be absorbed, than the ones taking a direct path. The selective absorption of the long lived photons results in a negative phase shift of the modulated light.

5.2 Conclusion

The idea of using phase-resolved measurements to detect small tumours in breast tissue is promising. Even though a simple experimental setup was used for this project, it was possible to detect variations in the optical properties of the tissue phantom. The results from the numerical calculations were interesting. The conclusion drawn from the experiments must, however, be that a homodyne approach to phase-resolved transillumination is difficult to accomplish. An increased understanding for the method itself has, however, come out of the project, which will make it easier to continue the work in our lab. to find an efficient phase-resolved transillumination method. A heterodyne detection method, such as the cross-correlation method described in chapter 1.3.5.3, will now be considered.

5.3 The Future

Some kind of scanning equipment has to be developed, before it will be possible to clinically use an equipment similar to the one described in this paper. As the time aspect of the investigation is important, it would be desirable to make a whole image in one measurement, just like in mammography. A possible approach could be to use a CCD array detector in conjunction with a modulated image intensifier (see Ref. [32]). As mentioned earlier, it is also important to investigate the optical properties of tissue, before being able to fully develop any transillumination method.

6 Acknowledgements

First of all I would like to thank my supervisors Claes af Klinteberg and Stefan Andersson-Engels, who have guided me throughout my work.

Then I would like to thank all the Diploma workers at the division for cheering me up when needed, and for helping me with computer problems.

I would like to thank Anne Lunné for showing me the work at Sankt Lars Mammography Centre.

I would also like to thank Alan Sabirsh for helping me with the proof-reading.

Finally I would like to thank everybody at the Department of Atomic Physics who have helped me with problems during my experiments.

7 References

1. B. Ween, C. van der Lelie, J.B. Olsen, J.B. Reitan, E.M. Sager, S. Thoresen and A. Widmark, "*Mammografi*", Universitetsforlaget AS, Oslo, 1992, (in Norwegian).

2. Statens Strålskyddsinstitut, "Om Hälsoundersökning med Mammografi", Information Folder in Swedish, Tryckhuset Linköping.

3. O. Jarlman, "Diagnostic Transillumination of the Breast", Dissertation Thesis, University Hospital, Lund, 1991.

4. H. Noltenius, *Human Oncology*, Urban & Schwarzberger, Baltimore - Munich, 1981.

5. M. Swift, D. Morell, R.B. Massey, and C.L. Chase, "Incidence of Cancer in 161 Families Affected by Ataxia-Telangiectasia", N. Engl. J. Med. **325**:1831-1836, 1991.

6. R. Bernro and I. Pettersson, "Electromagnetic Waves in Tissue", Diploma Paper, Lund Institute of Technology, 1987.

7. A. Lunné, Sankt Lars Mammography Center, Private communication, 1995.

8. H.J. Isard, "Other Imaging Techniques", Cancer **53**:658-664, 1984.

9. B.C. Wilson and S.L. Jacques, "Optical Reflectance and Transmittance of Tissues: Principles and Applications", IEEE J. Quant. Electr. **26**:2186-2199, 1990.

10. S. Andersson-Engels, R. Berg and S. Svanberg, "Effects of Optical Constants on Time-Gated Transillumination of Tissue and Tissue-Like Media", J. Photochem. Photobiol., B:Biol. **16**:155-167, 1992.

11. B. Ohlsson, J. Gundersen and D-M. Nilsson, "Diaphanography: A Method for Evaluation of the Female Breast", World J. Surg. **4**:701-707, 1980.

12. S. Andersson-Engels, R. Berg, S. Svanberg and O. Jarlman, "Time-Resolved Transillumination for Medical Diagnostics", Opt. Lett. **15**:1179-1181, 1990.

13. R. Berg, O. Jarlman and S. Svanberg, "Medical Transillumination Imaging Using Short-Pulse Diode Lasers", Appl. Opt. **32**:574-579, 1993.

14. S. Fantini, M.A. Franceschini, J.B. Fishkin, B. Barbieri and E. Gratton, "Quantitative Determination of the Absorption Spectra of Chromophores in Strongly Scattering Media: a Light-Emitting-Diode Based Technique", Appl. Opt. **33**:5204-5213, 1994.

15. J.R. Lakowicz, G. Laczko, I. Gryczynski, H. Szmacinski, W. Wiczk and M.L.Johnson, "Frequency-Domain Fluorescence Spectroscopy; Principles, Biochemical Applications and Future Developments", Ber. Bunsenges. Phys. Chem. **93**:316-327, 1989.

16. B.A. Feddersen, D.W. Piston and E. Gratton, "Digital Parallel Acquisition in Frequency Domain Fluorimetry", Rev. Sci. Instrum. **60**:2929-2936, 1989.

17. J.M. Schmitt, A.Knüttel and J.R. Knutson, "Interference of Diffusive Lightwaves", J. Opt. Soc. Am. A **9**:1832-1843, 1992.

18. B. Chance, K. Kang, L. He, J. Weng and E. Sevick, "Highly Sensitive Object Location in Tissue Models with Linear In-Phase and Anti-Phase Multi-Element Optical Arrays in One and Two Dimensions", Med. Sci. **90**:3423-3427, 1993.

19. K. A. Kang and B. Chance, "Phase and Intensity Information in a Highly Scattering Medium with Two Absorbers Using Phased Array Spectroscopy: Theoretical Study", SPIE **2082**:141-151, 1994.

20. B.W. Pouge and M.S. Patterson, "Perturbation Calculations of Photon Density Waves Interfering in an Inhomogenous Tissue-Simulating Medium", (manuscript).

21. S. Ertefai and E. Profio, "Spectral Transmittance and Contrast in Breast Diaphanography", Med. Phys. **12**:393-400, 1985.

22. C. af Klinteberg, "Studies of intensity Modulated Light in Turbid Media", Diploma Paper, Lund Institute of Technology, **LRAP-139**, 1993.

23. S.L. Jacques, "Priciples of Phase-Resolved Optical Measurements", Proc. SPIE Future Trends in Biomedical Applications of Lasers, SPIE **1527**:143-153, 1991.

24. S. Svanberg, *Atomic and Molecular Spectroscopy*, 2nd ed., Springer-Verlag, 1992.

25. A. Ishimaru, *Wave Propagation and Scattering in Random Media*, Academic Press, New York, 1978.

26. M.S. Patterson, B.C. Wilson and D.R. Wyman, "The Propagation of Optical Radiation in Tissue 1. Models of Radiation Transport and their Application", Lasers Med. Sci. **6**:155-168, 1991.

27. J. B. Fishkin and E. Gratton, "Propagation of Photon-Density Waves in Strongly Scattering Media Containing an Absorbing Semi-Infinite Plane Bounded by a Straight Edge", Opt. Soc. Am. **1**:127-140, 1993.

28. M.S.Patterson, S.J. Madsen, J.D. Moulton and B.C. Wilson, "Diffusion Equation Representation of Photon Migration in Tissue", IEEE MTT-S Digest **4**:905-908, 1991.

29. E. Gratton, W.W. Mantulin, M.J. vande Ven, J.B. Fishkin, M.B. Maris and B. Chance, "Imaging of Tissues Using Intensity-Modulated Near-InfraredLight", Science, (manuscript).

30. H.J. van Staveren, C.J.M. Moes, J. van Mark, S.A. Prahl and M.J.C. van Gemert, "Light Scattering in Intralipid-10% in the Wavelength Range of 400-1100 nm", Appl. Opt. **31**:4507-4514, 1991.

31. C. Lindquist, "Numerical Diffusion Modelling of Light in Turbid Media for Medical Diagnosis", Diploma Paper, Lund Institute of Technology, **LRAP-157**, 1994.

32. K.W. Berndt and J.R. Lakowicz, "Detection and Localization of Absorbers in Scattering Media Using Frequency Domain Principles", Proc. SPIE Time-Resolved Spectroscopy and Imaging of Tissues, SPIE **1431**:149-160, 1991.